Electronic Supplementary Material (ESI) for ChemComm.

SUPPLEMENTARY INFORMATION

Hyper-expanded interlayer separation in superconducting barium intercalated FeSe

K.V. Yusenko[a,b], J. Sottmann[b], H. Emerich[c],

W.A. Crichton[d], L. Malavasi[e] and S. Margadonna*[a]

[a] College of Engineering, University of Swansea, SA2 8PP, Swansea, UK

[b]Department of Chemistry, Centre for Materials Science and Nanotechnology, University of Oslo, PO Box 1033 Blindern, N-0315 Oslo, Norway.

[c]Swiss–Norwegian Beamlines, The European Synchrotron Radiation Facility, BP 220, Grenoble, 38043, France.

[d]The European Synchrotron Radiation Facility, BP 220, Grenoble, 38043, France.

[e]Department of Chemistry and INSTM, University of Pavia, Pavia 27100, Italy

email: s.margadonna@swansea.ac.uk

Materials synthesis. Starting β-FeSe has been synthesized from the elements: a mixture of Fe and Se fine powders (both were obtained from Alfa Aesar, chemical grade) were mixed in Mini-Mill PULVERISETTE 23 (10 ml stainless steel grinding bowls, 10 mm stainless steel grinding ball, 10 min), pressed into ø 10 mm pallet and sealed in vacuum inside a double-walled quartz tube. The tube has been annealed at 950-1070 °C during 48-50 h and quenched to 410 °C, followed by tempering over 100-110 h. The final material has been quenched into ice water, opened in a glove-box, lightly ground, and characterized using PXRD and SQUID. All samples of β-FeSe have hexagonal α-FeSe as minor admixture (<5 mass. %) and have $T_c = 8(1)$ K.

Synthesis of intercalated phases has been performed using a Schlenk-line modified for working with gaseous ammonia (Fig. S1). All operations were performed in evacuated or an ammonia-filled line and in an Ar-filled glove-box (mbraun LABmaster sp). Oxygen and water levels never reached more than 0.1 ppm. Liquid ammonia has been condensed using a dry ice – acetone cold bath (195 K). After the complete evacuation of the system, ammonia gas (compressed ammonia from steel cylinder, AGA, 5.0) has been first condensed in to the flask with 10-15 mg of lump Na (Sigma-Aldrich) for purification of residual water and oxygen and then carefully recondensed into the reaction flask or autoclave. Initial condensation of 20-30 ml of liquid ammonia needs approximately 10 minutes.

Low-temperature reaction (LT) has been performed in a round-bottom flask with a glass covered stirrer (Fig S1). 50 mg (0.37 mmol) of β-FeSe powder has been placed with a stoichiometric amount of Ba (Sigma-Aldrich, 5-15 mg 0.04-0.2 mmol). The composition has been varied between $Ba_{0.2}Fe_2Se_2$ and $Ba_{0.8}Fe_2Se_2$. After 5-10 min, the reaction mixture changed color from violet to green and finally to dark black. The solvent has been recondensed back into the first round flask after 2-12 h. The reaction mixture has then been dried in vacuum for 10-15 min at room temperature and transported inside a glove-box for any further manipulation and sample preparation. Typical diffraction profiles of obtained specimens are shown in Fig. S2.

The same scheme has been used for sealing the samples for magnetization measurements which were performed on a Quantum Design MPMS magnetometer. For these, the left-hand flask has been replaced with a quartz tube which was connected using PTFE High Vacuum screw cap joints. β-FeSe powder and Ba pieces were placed into quartz ampules (internal diameter 1.3 mm). 1-2 ml of solid ammonia was then condensed using liquid nitrogen and then the tube was evacuated and sealed. After sealing the tube was placed into dry ice - acetone bath and then inserted into the MPMS measurement chamber.

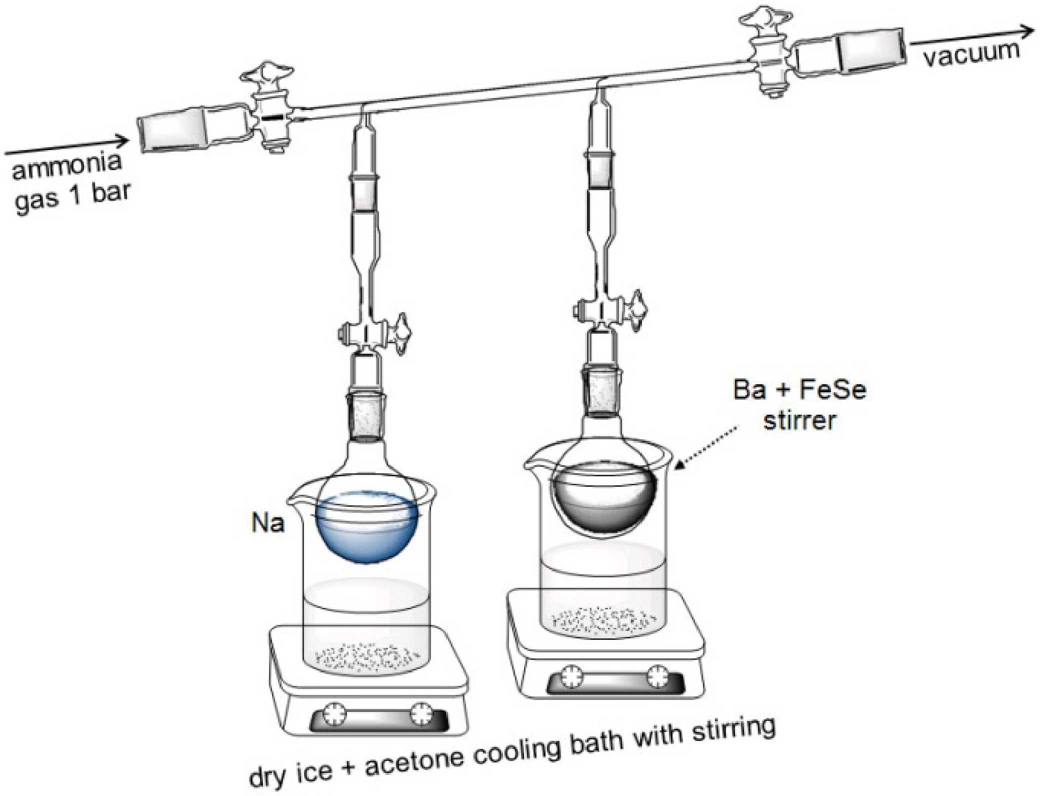

Figure S1. Drawing of LT experimental set up used in this work.

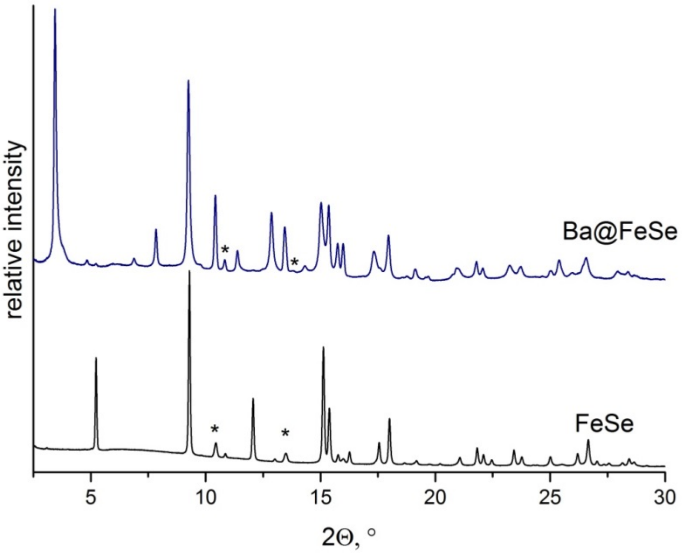

Figure S2. Typical synchrotron X-ray diffraction profiles for LT-synthesised Ba@FeSe intercalates (λ = 0.5048 Å, 300 K). Asterisks denote the Bragg reflections corresponding to the hexagonal α-FeSe minority phase.

Room temperature reaction (RT) was performed in stainless steel laboratory autoclave from ROTH (Model 0, 50 ml) with a glass liner. 100 mg (0.74 mmol) of β-FeSe fine powder has been placed into the glass insert together with glass covered stirrer and stoichiometric amount of Ba lump 5-15 mg (0.08-0.4 mmol) has been fastened on the insert's wall in the middle. The reactor was connected to the Schlenk-line and evacuated. Liquid ammonia was re-condensed in the same manner; reactor was closed and kept with stirring at room temperature (24-25 °C) during 2-4 days. Pressure inside the reactor reached 8 bar which is in concordance with a vapor pressure of liquid ammonia at room temperature. After the reaction, the autoclave has been cooled with dry ice – acetone cold bath, ammonia was carefully re-condensed and after drying in vacuum for 10-15 min was transported inside glove-box. All experiments with gaseous and liquid ammonia should be performed with care under fumehoods.

The LT and RT reactions lead to the isolation of a single tetragonal phase with a characteristic *d* spacing of ~ 8.4 Å, independently of the initial nominal composition and reaction time. This phase, identified as Phase VI in the manuscript, is always obtained upon evacuation of the original reaction mixture. Rietveld refinements of the X-ray powder diffraction data obtained on different batches of Phase VI (synchrotron and laboratory) always give an estimated composition of $Ba_{0.3}Fe_2Se_2$ (see for example Table S5). Elemental analysis was performed twice on one of these samples by an external laboratory using a Perkin Elmer AAS AAnalyst 200 (Mikroanalytisches Laboratorium KOLBE: www.mikro-lab.de). The resulting composition of $Ba_{0.30}Fe_{1.64}Se_{2.00}$ was obtained, in very good agreement with the values obtained by Rietveld refinements.

Synchrotron X-ray powder diffraction.

Measurements were all performed at BM1B Swiss-Norwegian beam line at The European Synchrotron Radiation Facility. Different samples obtained by the LT and RT reaction routes were sealed in 0.5 mm diameter thin-wall glass capillaries and diffraction profiles were recorded at various temperatures ranging between 80 and 300 K (λ = 0.5048 Å) using the Dexela 2923 CMOS 2D detector.

For the *in situ* experiments the principal scheme (Fig. S3) includes 1.3 mm quartz capillary connected to the gas line. 5-10 mg of β-FeSe powder has been placed inside 1.3 mm capillary separately from small piece of metallic Ba (1-5 mg). The capillary was closed inside the glove-box and connected to the ammonia gas line. The capillary was then pre-cooled to 200 K using a cryo-stream after opening of the capillary to the gas line filled with 2 bar ammonia gas. Diffraction patterns were collected after 2 min 12 times per minute using the 2D detector. Si and LaB_6 external standards were used for wavelength and detector position calibration. For data reduction the FIT2D software (A. P. Hammersley, S. O. Svensson, M. Hanand, A. N. Fitch, and D. Hausermann, High Press. Res. 14, 235 (1996)) was used. Experiments were performed in experimental hutch with ventilation and equipped with NH_3 gas sensor placed close to the reaction vessel

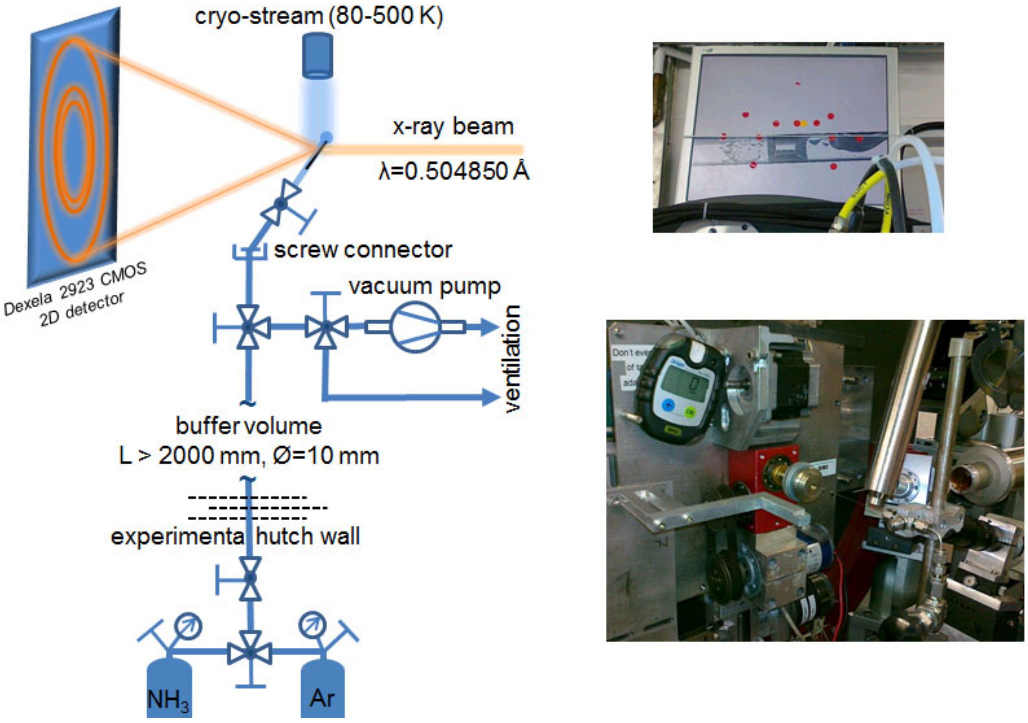

Figure S3. Schematic drawing of the *in situ* experimental set up used at SNBL-BM1B beamline (ESRF) for temperature and time resolved X-ray diffraction experiments.

Two series of experiments were performed. In the first, serial diffraction patterns were collected at a constant temperature of 200 K during 12 h. The 2000 individual profiles were analyzed using TOPAS V5.0. Software package (Bruker AXS (2011). TOPAS, V5.0. (Computer Software), Bruker AXS, Karlsruhe, Germany). For each individual data set, zero-shift, background, cell parameters, Ba-site occupancies, peak-profile parameters for three phases (β-FeSe, Phase I, Phase II), as well as their weight fractions, were refined simultaneously. Weight fractions depend on the time and their time dependences can be fitted using the first order reaction kinetic (β-FeSe $\xrightarrow{\text{reaction a}}$ Phase I $\xrightarrow{\text{reaction b}}$ Phase II; however, reaction rates should also depend on the Ba composition, which was constant during the reaction). Weight fractions of β-FeSe and Phase II can be fitted using exponential functions $W(t) = W_0+W\cdot e^{-kt}$ (where W_0, W, and k – constants specific for each curve, t – time). $k_a/k_b \approx 25\text{-}30$, which allow for analysis of the reactions independently of each other.

The second set of experiments was performed at variable temperature following different heating and cooling protocols between 80 and 300 K. Representative diffraction profiles have been extracted and analyzed. Initial evaluation and differential Fourier map analysis was performed with the Jana2006 software (Petricek, V., Dusek, M. & Palatinus, L.

(2014). Z. Kristallogr. 229(5), 345-352; V. Petricek, M. Dusek, L. Palatinus, Jana2006. The crystallographic computing system. Institute of Physics. Praha, Czech Republic. 2006; http://www.xray.fzu.cz/jana/jana.html). For the final Rietveld refinements the GSAS software package was used (A.C. Larson and R.B. Von Dreele, "General Structure Analysis System (GSAS)", Los Alamos National Laboratory Report LAUR 86-748 (2000). B. H. Toby, EXPGUI, a graphical user interface for GSAS, J. Appl. Cryst. 34, 210-213 (2001).)

Data have been indexed in the *I*4/*mmm* space group for Phases I, II and VI based on the model proposed, for example, for ammonia-poor $Li_{0.6}(NH_2)_{0.2}(NH_3)_{0.8}Fe_2Se_2$ (M. Burrard-Lucas et al., Nat. Mater., 2013, 12, 15.) and in the *P*4/*nmm* (setting 2) space group for Phases III, IV, and V based on the ammonia-rich $Li_{0.6}(NH_2)_{0.2}(NH_3)_{1.8}Fe_2Se_2$ described by S.J. Sedlmaier et al. (JACS, 2014, 136, 630−633). For the refinement, cell parameters, background, and line profile parameters, atomic coordinates and occupancies (Ba and N) were refined simultaneously. In all case hexagonal α-FeSe was found as a secondary phase. Also, depending on temperature and stage of the reaction additional lines were present in the diffraction profiles corresponding to different phases arising from the direct reaction of Ba with NH_3 (e.g. $Ba(NH_2)_2$). The Bragg reflections of these phases disappear after enough ammonia has been condensed in the capillary. The unit cell parameters of Phase V were obtained with Le Bail refinements considering *P4/nmm* symmetry

Magnetic susceptibility measurements were carried out in both ZFC and FC modes between 4 and 55 K in a field of 10 Oe (Magnetic Property Measurement System, Quantum Design).

For *in situ* monitoring mixtures of β-FeSe and Ba were placed into quartz tube, 0.5-1.5 ml of solid ammonia was condensed using liquid nitrogen as cooling agent and sealed after evacuation. Reaction between β-FeSe and Ba does not occur in solid ammonia and the mixture could then be transferred into the measurement chamber. The starting frozen mixture show only a presence of β-FeSe with T_c = 8 K. Blank experiment (β-FeSe + NH_3) shows no influence of solid NH_3 on the behavior of β-FeSe, and there was no evident reaction between compounds.

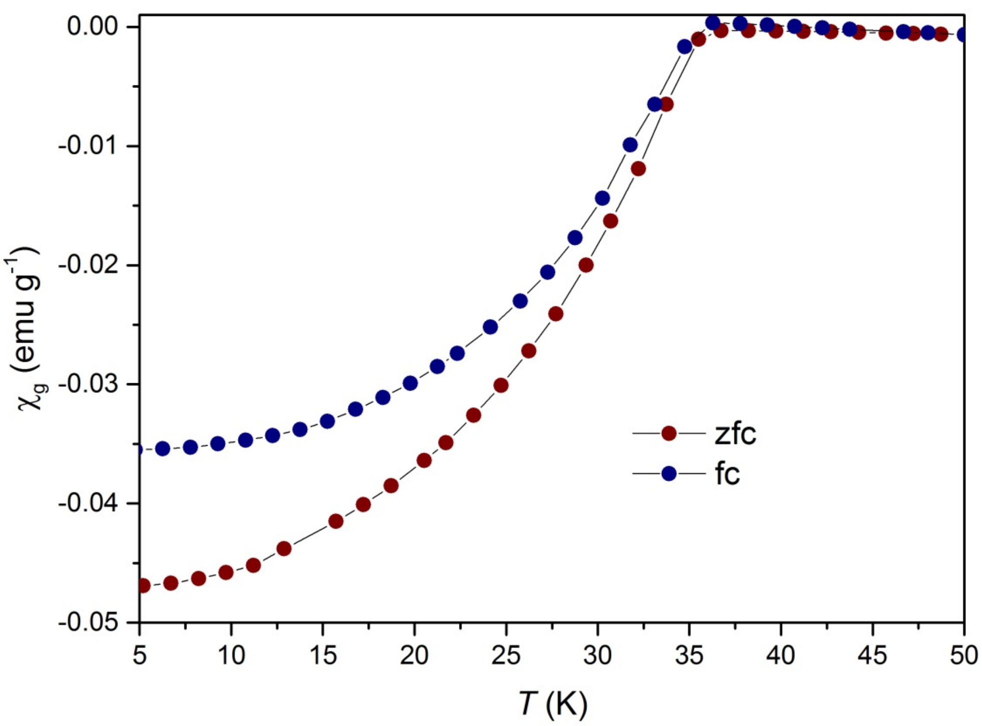

Figure S4. The magnetization curves for Phase VI with the zero-field-cooling (zfc) and field-cooling (fc) modes at H = 10 Oe.

Crystallographic information:

Table S1. Refined parameters for Phase I as obtained by Rietveld refinement of the synchrotron X-ray powder diffraction data ($\lambda = 0.5048$ Å, 200 K) in the space group *I*4/*mmm* with unit cell parameters, $a = 3.8110(2)$ Å and $c = 26.249(2)$ Å (agreement factors: $R_{wp} = 7.53\%$, $R_{exp} = 5.61\%$).

Atom	*n*	*x*	*y*	*z*	Site	B_{iso} (Å^2)
Se	1	1/2	1/2	0.1973(2)	*4e*	0.76(4)
Fe	1	1/2	0	1/4	*4d*	1.04(5)
Ba	0.143(4)	0	0	0.0872(5)	*4e*	2.6(7)
N	0.35(5)	0	0	1/2	*2b*	6.3(7)

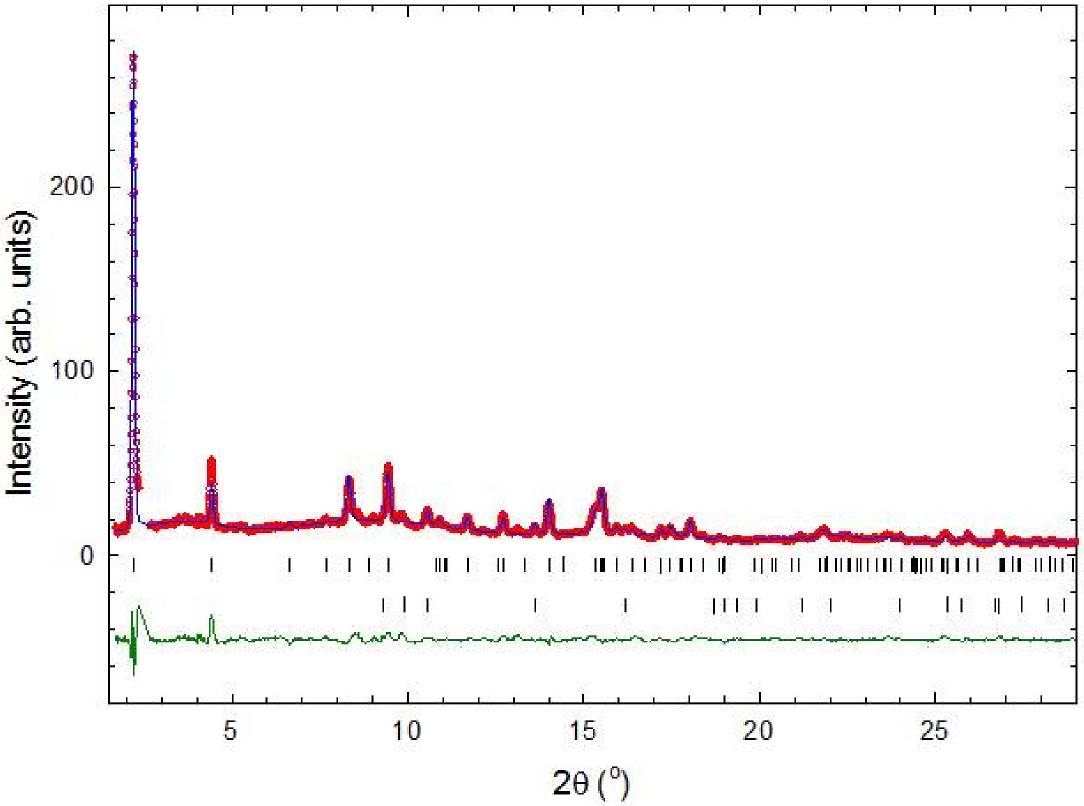

Figure S5. Final observed (°) and calculated (|) synchrotron X-ray diffraction profiles (λ= 0.5048 Å) for Phase I at 200 K. The lower solid line is the difference profile and the tick marks show the reflection positions. Small impurity peaks corresponding to α-FeSe are also present in the diffraction profile. The excluded region corresponds to a shoulder on the left of the 002 Bragg reflection which indicates the beginning of the transformation to Phase II.

Table S2. Refined parameters and selected bond distances for Phase II as obtained by Rietveld refinement of the synchrotron X-ray powder diffraction data (λ = 0.5048 Å, 200 K) in the space group *I*4/*mmm* with unit cell parameters, a = 3.8530(2) Å and c = 23.037(1) Å (agreement factors: R_{wp} = 7.81%, R_{exp} = 5.03%).

Atom	n	x	y	z	Site	B_{iso} (Å^2)
Se	1	1/2	1/2	0.1877(2)	*4e*	0.72 (5)
Fe	1	1/2	0	1/4	*4d*	1.71(5)
Ba	0.243(4)	0	0	0.5	*2b*	2.3(7)
N	0.96(3)	0	0	0.0627(9)	*4e*	6.5(7)

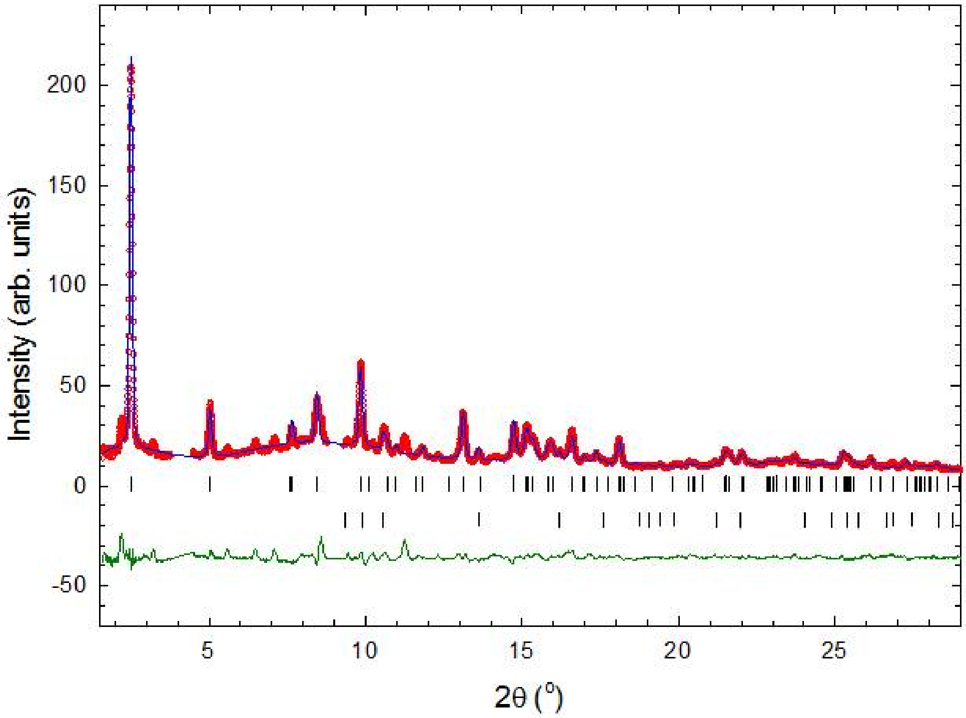

Figure S6. Final observed (°) and calculated (|) synchrotron X-ray diffraction profiles (λ= 0.5048 Å) for Phase II at 200 K. The lower solid line is the difference profile and the tick marks show the reflection positions. Small impurity peaks corresponding to α-FeSe are also present in the diffraction profile. The excluded region corresponds to unknown Ba-NH_3 phases which form at the beginning of the reaction.

Table S3. Refined parameters and selected bond distances for Phase III as obtained by Rietveld refinement of the synchrotron X-ray powder diffraction data ($\lambda = 0.5048$ Å, 250 K) in the space group *P*4/*nmm (origin choice 2)* with unit cell parameters, $a = 3.7864(4)$ Å and $c = 11.0889(7)$ Å (agreement factors: $R_{wp} = 6.17\%$, $R_{exp} = 4.82\%$).

Atom	n	x	y	z	Site	B_{iso} (Å^2)
Se	1	1/4	1/4	0.3686(8)	*2c*	4.3(3)
Fe	1	3/4	1/4	1/2	*2b*	3.5(2)
Ba	0.174(4)	3/4	3/4	0.067(2)	*2b*	4.8(6)
N	0.53(3)	1/4	3/4	0.789(4)	*4f*	5.2(6)

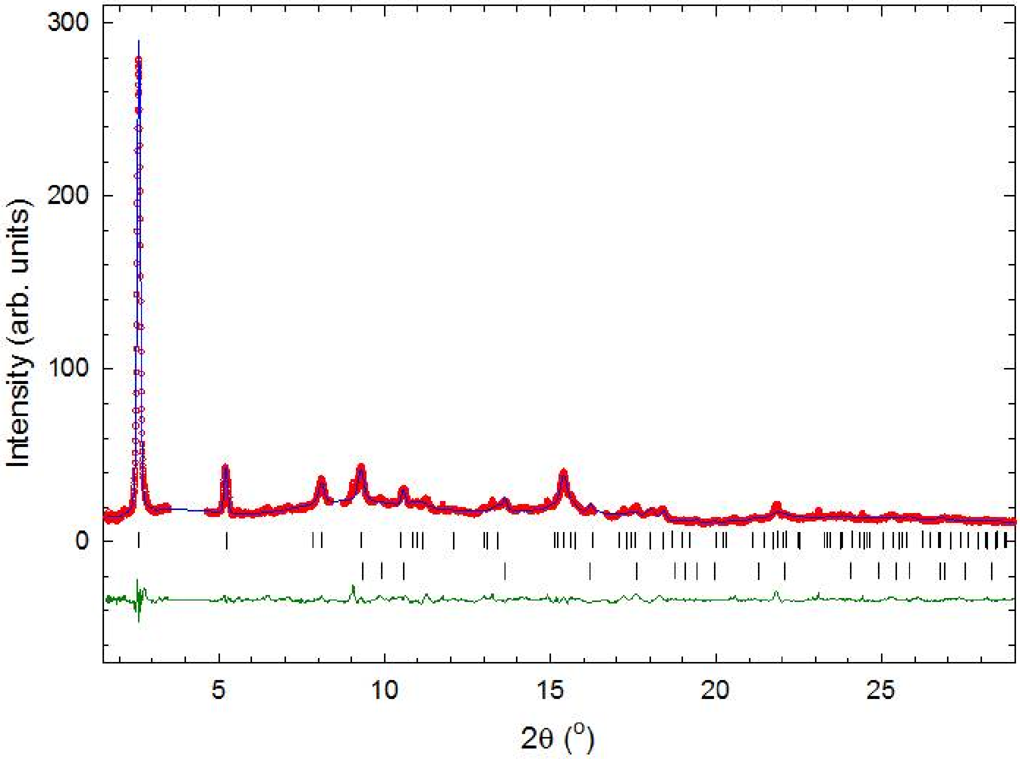

Figure S7. Final observed (°) and calculated (|) synchrotron X-ray diffraction profiles (λ= 0.5048 Å) for Phase III at 250 K. The lower solid line is the difference profile and the tick marks show the reflection positions. Small impurity peaks corresponding to α-FeSe are also present in the diffraction profile. The excluded region corresponds to unknown Ba-NH_3 phases which form at the beginning of the reaction.

Table S4. Refined parameters and selected bond distances for Phase IV as obtained by Rietveld refinement of the synchrotron X-ray powder diffraction data (λ = 0.5048 Å, 300 K) in the space group *P4/nmm (origin choice 2)* with unit cell parameters, a = 3.8058(4) Å and c = 9.059(1) Å (agreement factors: R_{wp} = 8.23%, R_{exp} = 5.99%).

Atom	n	x	y	z	Site	B_{iso} (Å^2)
Se	1	1/4	1/4	0.3341(6)	*2c*	2.2(1)
Fe	1	3/4	1/4	1/2	*2b*	1.8(1)
Ba	0.187(5)	3/4	3/4	0.071(1)	*2c*	2.4(9)
N	0.26(2)	1/4	3/4	0.895(7)	*4f*	5.8(9)

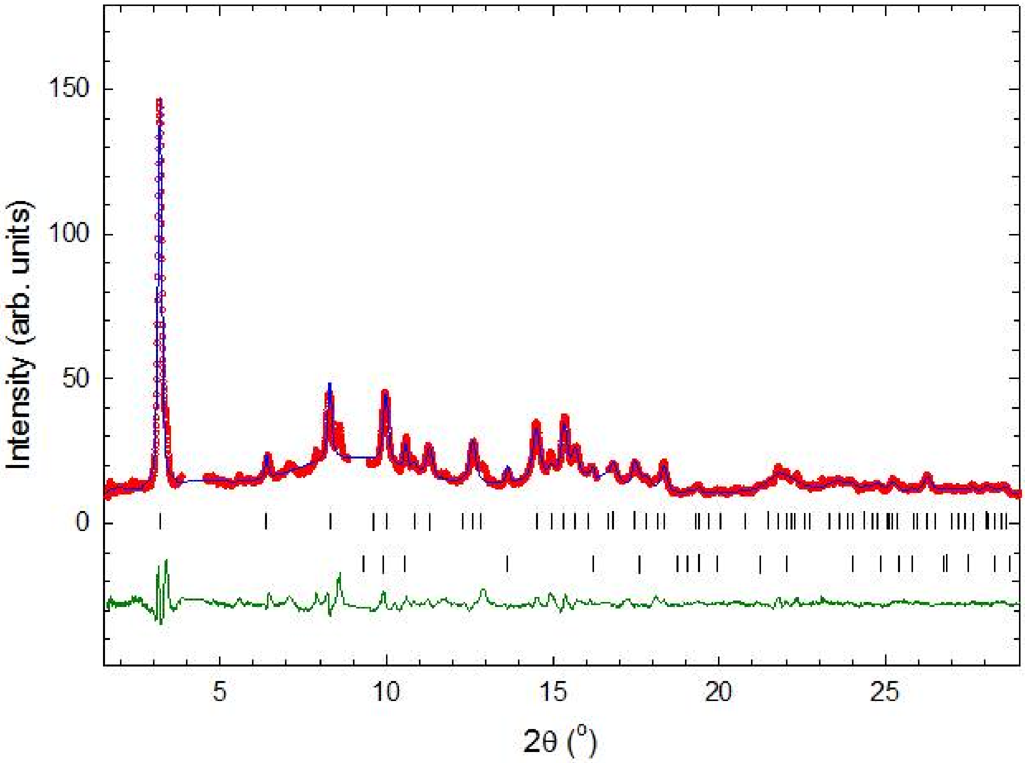

Figure S8. Final observed (°) and calculated (|) synchrotron X-ray diffraction profiles (λ= 0.5048 Å) for Phase IV at 300 K. The lower solid line is the difference profile and the tick marks show the reflection positions. Small impurity peaks corresponding to α-FeSe are also present in the diffraction profile. The excluded region corresponds to unknown Ba-NH_3 phases which form at the beginning of the reaction.

Table S5. Refined parameters and selected bond distances for Phase VI as obtained by Rietveld refinement of the synchrotron X-ray powder diffraction data (λ = 0.5048 Å, 300 K) in the space group *I*4/*mmm* with unit cell parameters, *a* = 3.7786(1) Å and *c* = 16.724(1) Å (agreement factors: R_{wp} = 6.36%, R_{exp} = 4.72%).

Atom	*n*	*x*	*y*	*z*	Position	B_{iso} (Å^2)
Se	1	0	0	0.3399(2)	*4e*	0.77(6)
Fe	1	0	0.5	1/4	*4d*	0.80(9)
Ba	0.280(5)	0	0	0	*2a*	2.8(5)

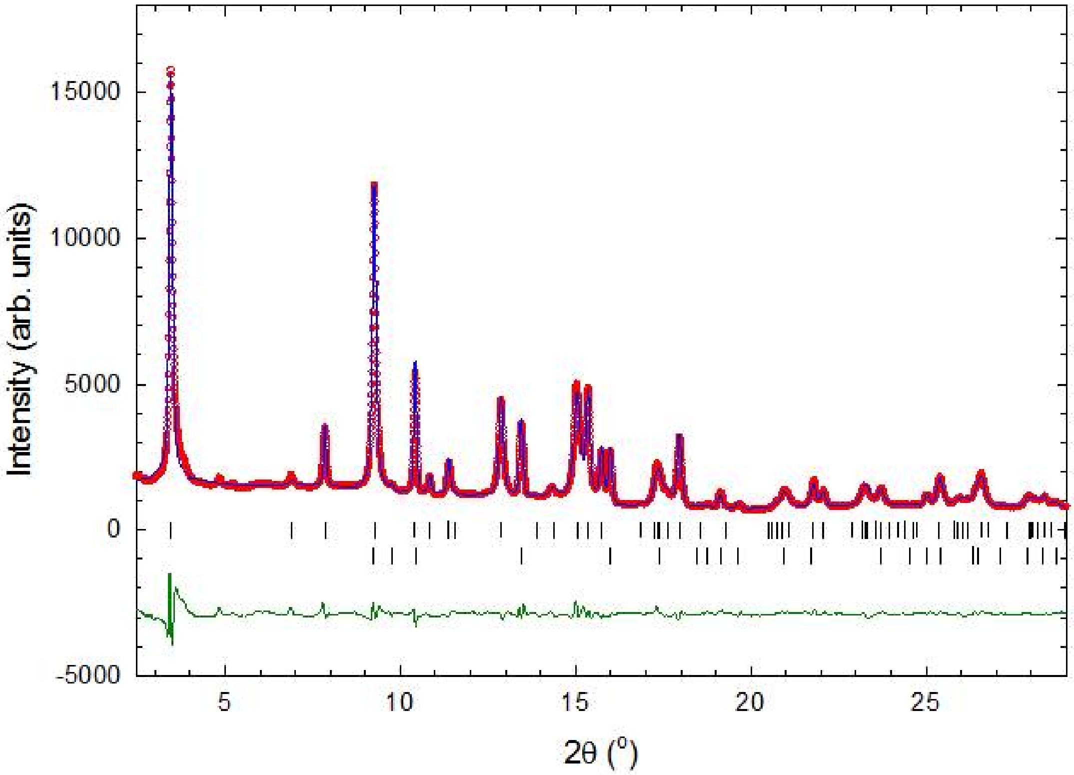

Figure S9. Final observed (°) and calculated (|) synchrotron X-ray diffraction profiles (λ= 0.5048 Å) for Phase VI at 300 K. The lower solid line is the difference profile and the tick marks show the reflection positions. Small impurity peaks corresponding to α-FeSe are also present in the diffraction profile.